Int. J. Multiphase Flow Vol. 8, No. 4, pp. 443–447, 1982
Printed in Great Britain.

0301–9322/82/040443–05$03.00/0
Pergamon/Elsevier

BRIEF COMMUNICATION

PRESSURE FLUCTUATIONS AND FLOW PATTERN RECOGNITION IN VERTICAL TWO PHASE GAS–LIQUID FLOWS

NARINDER K. TUTU
Department of Nuclear Energy, Brookhaven National Laboratory, Upton, NY 11973, U.S.A.

(*Received* 3 *July* 1981; *in revised form* 7 *February* 1982)

1. INTRODUCTION

Two phase gas–liquid flows play an important role in advanced energy conversion systems, large industrial chemical reactors, and diverse systems such as oil gas pipe lines and nuclear reactors. The quantities of engineering interest, for example: average pressure drop, heat transfer rates, rates of chemical reaction, depend strongly on the type of flow regime. Thus the need for mathematical modelling of these flows demands greater understanding of the physics of the flow, and also the ability to predict the flow regimes.

Flow pattern maps based on visual observations have been developed by various investigators and from the basis for predicing flow regimes. A review and assessment of many such maps was recently published by Savery (1980). By replotting the flow pattern maps of various investigators on a set of common coordinates, Dukler & Taitel (1977) have shown that there is little agreement among the various published maps. As they have indicated, part of the reason for this discrepancy is the subjectivity of the observer involved in distinguishing between the various flow regimes. Thus there is a need to develop objective methods for flow pattern recognition.

One of the first attempts in this direction has been that of Hubbard & Dukler (1966) who used the spectra of wall pressure fluctuations to discriminate between various flow regimes in the case of horizontal flows. Jones & Zuber (1975) used the probability density function (PDF) of the instantaneous void fraction to differentiate between the various flow regimes. However, this technique is of limited value since powerful X-ray or γ-ray sources are needed. Their experiments were carried out in a channel less than 5 mm deep; for ducts that are large (say > 150 mm deep) this method will be prohibitively expensive and hazardous. More recently, Barnea *et al.* (1980) have used an electrical conductance probe for flow pattern recognition. Although the technique involves subjective viewing of the raw signal (which is basically the local phase density function), the method seems promising.

In what follows, measurements of wall pressure fluctuations and pressure drop fluctuations are presented for the flow regimes of bubbly, slug, churn, and annular type. It is seen that these measurements can readily be used for flow pattern recognition.

2. EXPERIMENTAL SET UP

Figure 1 shows the schematic of the air water loop that was used for the present measurements. The test section is a 52.2 mm inside diameter (D) clear PVC pipe. Flexible couplings were installed at various points in the loop to isolate the test section from the vibrations induced by the pump. Air was injected through a porous plate in the "Mixer" during the first six runs, and directly by a 25 mm diameter pipe during the last two runs when the air flow rates were very large. A heat exchanger was included in the loop to maintain isothermal conditions (within ± 0.1°C) during the experiment. Two Endevco Model 8506-5 piezoresistive

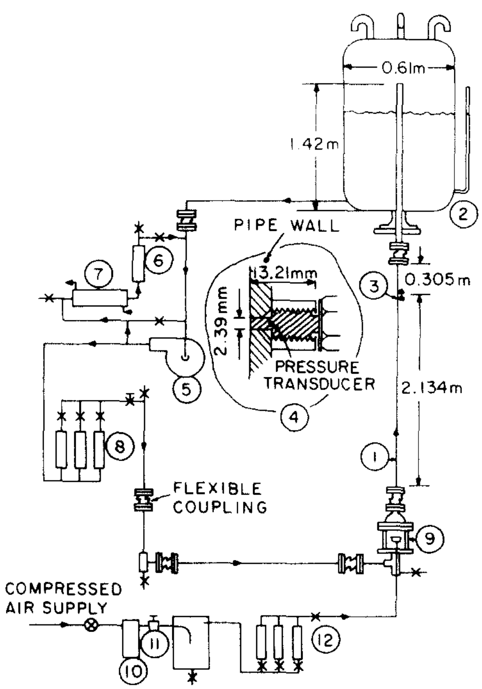

Figure 1. Schematic of the air–water loop: 1, test section; 2, air separator; 3, pressure transducers; 4, mounting detail of pressure transducer; 5, pump; 6, flow meter, 7, heat exchanger; 8, flow meters; 9, mixer; 10, filter; 11, regulator; 12, flow meters.

pressure transducers separated axially by D/2 were mounted flush with the inside pipe wall along the same vertical axis. These transducers have a resonance frequency of 65 kHz.

Analog signals from the pressure transducers were recorded on a magnetic tape using the Honeywell Model 96 tape recorder. The frequency response at the tape speed selected during the recordings is from DC to 5 kHz (1 dB). NEFF System 620 and the HP 21 MX Series computer were used to digitize and process the pressure signals. Preliminary analog measurements of the spectra indicated little energy beyond 1 kHz. So the first six runs were digitized at the sampling rate of 3.2 kHz; the signals were low pass filtered at 1.6 kHz (−3 dB, 24 dB per octave) prior to sampling to prevent aliasing. The last two runs, which involved higher gas phase velocities, and thus higher frequencies, were digitized at 25 kHz. The total number of data points processed for each run was 0.2048×10^6 for the first six runs and 0.3072×10^6 for the last two runs.

3. RESULTS AND DISCUSSION

Let p_2 and p_1 be the pressure signals from the lower and upper pressure transducers respectively; the pressure drop signal (p_2–p_1) denoted by p_{21}, was generated simultaneously by using an analog "difference" circuit. Since the two transducers are only separated by a distance that equals the pipe radius, the time average value of the pressure drop, $\overline{p_{21}}$, is quite small. Due to the very low frequency drift in the DC offset of the transducers and the finite time lapse between the calibration of the transducers and the experimental run, $\overline{p_{21}}$ does not give the correct value of the average pressure drop. An estimate Δp for it was therefore calculated based on the time average $\overline{p_1}$ and the exit pressure at the end of the vertical pipe; the computed probability density function (PDF) of p_{21} was then simply shifted by the appropriate amount.

If x is a random variable with zero mean, its skewness factor S_x and flatness factor F_x are defined by:

$$S_x = \overline{x^3}/(\overline{x^2})^{3/2}, \quad F_x = \overline{x^4}/(\overline{x^2})^2.$$

For a Gaussian distribution $S_x = 0$, and $F_x = 3.0$.

Figures 2 and 3 show the PDF of the dimensionaless pressure drop $p_{21}^* = (p_2 - p_1)/(\Delta p)_h$ during the various flow regimes. $(\Delta p)_h$ is the hydrostatic pressure drop between the two transducers when only water is present in the test section. Photographs of the flow pattern for some of the experimental runs are shown in figure 4. The hydrostatic (or gravitational) contribution to p_{21}^* is of course bound between 0 and 1; thus any excursions outside this domain must be due to dynamic effects (accelerative, and wall friction). As expected, the bubbly flow regime exhibits a single peaked PDF (runs 1 and 2) centered around the neighborhood of $p_{21}^* = 1 - \alpha$; where α is the average void fraction. Runs 3 and 4 (figure 3) show that the PDF during the slug flow regime is bimodal; the smaller peak which corresponds to the passage of "Taylor bubbles" is located in the neighborhood of $p_{21}^* = 0$, and the larger peak which corresponds to the bubbly liquid slugs is located around $p_{21}^* = 1$. During the churn regime (runs 5 and 6) although the PDF remains bimodal the magnitude of the peaks is reversed, the larger peak now occurring at $p_{21}^* \approx 0$. This happens due to two reasons: first, the "Taylor bubbles" have now degenerated into longer and more frequently occurring gas "pockets"; this tends to increase the magnitude of the peak at $p_{21}^* = 0$, and secondly since the motion is more chaotic there is a much wider distribution of amplitudes below the second peak; this obviously tends to lower the PDF value of this peak. During the instances when a gas "pocket" is passing by the probes and the liquid film is travelling down the pipe, the instantaneous pressure drop, as seen from the PDFs, can be negative. This is consistent with the observations of Akagawa *et al.* (1971) during the slug flow. As the volumetric quality, β, is increased during the churn flow, the peak around $p_{21}^* = 1$ decreases in amplitude and moves toward the peak at $p_{21}^* = 0$, until at values of β approaching that during the annular flow this second peak completely disappears. This case is shown in figure 2 (run 7). Run 8 in the same figure shows the PDF for the case when the flow is annular but very close to the churn/annular transition. The Skewness has decreased by a factor of 2 (see table 1), and it is expected that at higher air flow rates the PDF should become even more symmetric. However, due to limitations of the compressor output, the air flow rate could not be increased further.

From the PDFs of the pressure drop signal p_{21} and the pressure signal p_1, moments up to 4th order were calculated. These results are summarized in Table 1. U_G and U_L are the superficial velocities of air and water respectively, and $'$ indicates the root mean square of the variable.

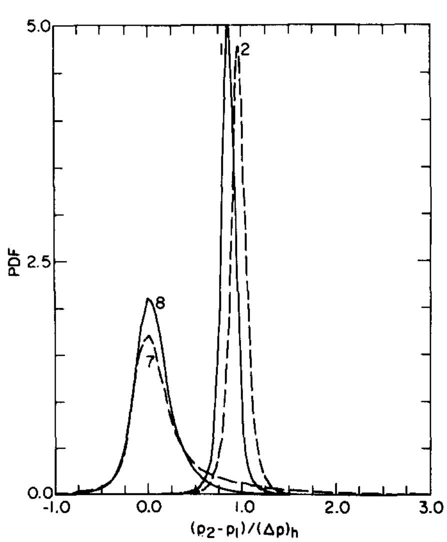

Figure 2.

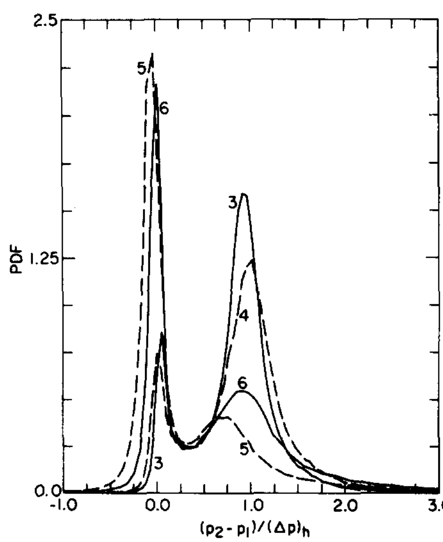

Figure 3.

Figure 2. Propability density function of the pressure drop. 1, Run 1; 2, run 2; 7, run 7; 8, run 8.

Figure 3. Probability density function of the pressure drop. 3, Run 3; 4, run 4; 5, run 5; 6, run 6.

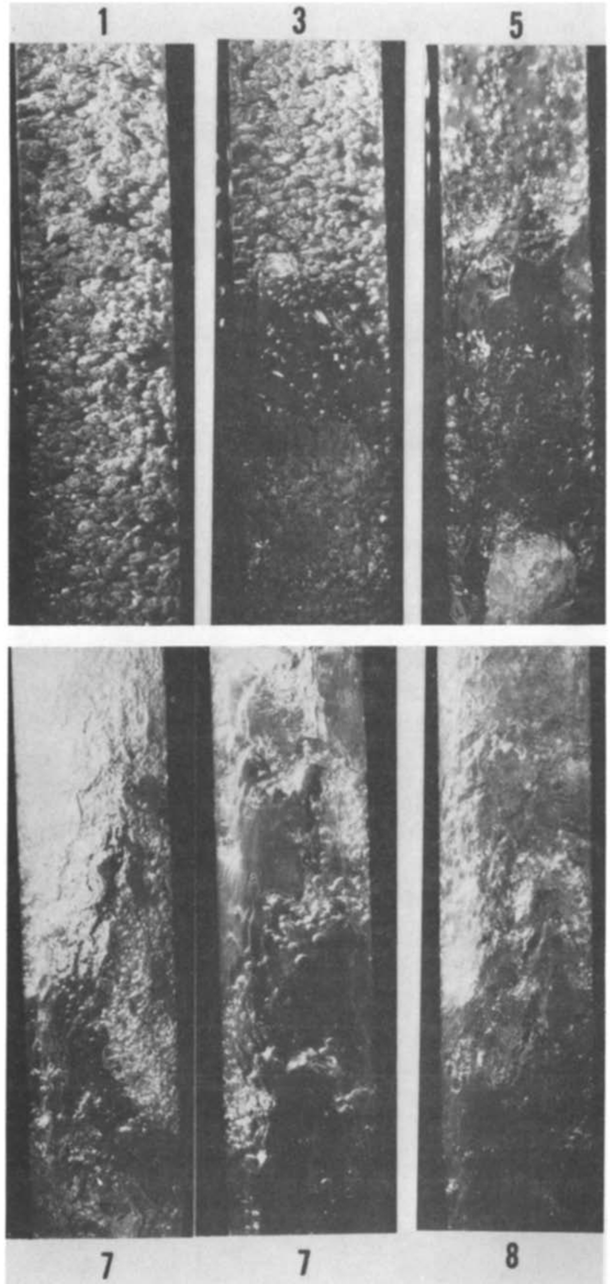

Figure 4. Photograph of the flow patterns. 1, Run 1; 3, run 3; 5, run 5; 7, run 7; 8, run 8.

Table 1. Moments of pressure fluctuations in vertical air–water flow

Run No.	U_G m/s	U_L m/s	β	$\frac{\Delta p}{(\Delta p)_h}$	$\frac{p_1}{(\Delta p)_h}$	$\frac{p_1}{\Delta p}$	S_{p_1}	F_{p_1}	$\frac{p_{21}}{(\Delta p)_h}$	$\frac{p_{21}}{\Delta p}$	$S_{p_{21}}$	$F_{p_{21}}$	Flow Regime
1	0.085	0.381	0.182	0.855	0.283	0.331	0.95	13.8	0.099	0.116	0.19	6.84	Bubbly
2	0.065	0.853	0.071	0.962	0.215	0.224	0.05	3.10	0.109	0.114	0.21	5.31	Bubbly
3	0.149	0.382	0.280	0.811	1.585	1.953	−0.16	2.96	0.442	0.544	0.18	4.67	Slug
4	0.217	0.874	0.199	0.864	1.733	2.005	−0.04	3.17	0.516	0.597	0.34	4.7	Slug
5	0.525	0.103	0.836	0.365	5.005	13.71	−0.18	2.83	0.734	2.012	2.60	14.2	Churn
6	0.623	0.834	0.428	0.672	4.120	6.133	−0.20	3.23	0.832	1.238	1.91	9.8	Churn
7	5.82	0.050	0.992	0.190	3.896	20.47	0.50	3.10	0.519	2.728	2.40	13.7	Churn
8	11.76	0.011	0.999	0.062	0.539	8.75	0.43	4.1	0.273	4.437	1.20	14.0	Annular

During the annular flow regime $p'_1/(\Delta p)_h$ is much smaller (almost by an order of magnitude) than that during the churn regime. This makes the task of discriminating between the flow regimes at very high values of void fraction (runs 7 and 8) easy.

4. CONCLUDING REMARKS

It has been shown that the PDF of the pressure drop signal together with the measurements of $p'_1/(\Delta p)_h$ and $S_{p_{21}}$ can be used objectively to discriminate between the various flow regimes in vertical two phase gas–liquid flows when the average pressure drop is mostly gravitational. This technique of flow pattern recognition, unlike the γ-ray or X-ray technique, is simple and applicable to large sized ducts without increase in cost or complexity.

Acknowledgements—The author greatfully acknowledges the help of Drs. Owen C. Jones and Nesim Abuaf in initiating this study. Assistance and encouragement from Dr. Abuaf during the phase which involved the evaluation of various types of pressure transducers proved valuable. Thanks are also due to Messrs. James Klein, John Klages, Donald Becker, and Eric Schwarz for the design and fabrication of the air-water loop, and to Mrs. Yako Sanborn for developing the software for data acquisition. This work was supported by the Division of Chemical Sciences, U.S. Department of Energy, Washington, D.C., under Contact No. DE-AC02-76CH00016.

REFERENCES

Akagawa, K., Hamaguchi, H., Sakaguchi, T., & Ikari, T. 1971 Studies on the fluctuation of pressure drop in two-phase slug flow. *Bull. JSME* **14**, 447–454.

Barnea, D., Shoham, O., & Taitel, Y., 1980 Flow pattern characterization in two phase flow by electrical conductance probe. *Int. J. Multiphase Flow* **6**, 387–397.

Dukler, A. E. & Taitel, Y., 1977 Flow regime transitions for upward gas liquid flow: a preliminary approach through physical modelling. Progress Report No. 1, NUREG-0162, NRC-2,4, University of Houston, Texas.

Hubbard, N. G., & Dukler, A. E., 1966 The characterization of Flow Regimes for Horizontal Two Phase Flow. *Proc.* 1966 *Heat Transfer and Fluid Mechanics Institute*, pp. 100–121. Stanford University Press, California.

Jones, O. C., & Zuber, N., 1975 The interrelation between void fraction fluctuations and flow patterns in two phase flow. *Int. J. Multiphase Flow* **2**, 273–306.

Savery, C. W., 1980 Flow Patterns in Two Phase Fluid Flow. *Proc. Symp. Polyphase Flow and Transport Technology San Francisco*, pp. 75–88. A.S.M.E.